International Journal of Engineering Inventions
e-ISSN: 2278-7461, p-ISSN: 2319-6491
Volume 15, Issue 9 [September 2026] PP: 101-107

Resilient Frequency Regulation in Low-Inertia Microgrids Under Communication Impairments via Data-Age-Aware DOB-MPC

Nguyen Duy Trung[1], Nguyen Thi Mai Duyen[1], Nguyen Quang Huy[2], Le Cong Viet[1], Nguyen Xuan Quynh[3]
[1]*Faculty of Automation, Artificial Intelligence and Intelligent Systems, Electric Power University, Hanoi, Vietnam*
[2]*Faculty of Electrical Engineering, Electric Power University, Hanoi, Vietnam*
[3]*School of Electrical and Electronic Engineering, Hanoi University of Industry, Hanoi, Vietnam*
Corresponding Author: trungnd@epu.edu.vn

ABSTRACT: *Communication impairment is often treated as an external networking issue in microgrid frequency-control studies, although stale measurements directly alter the closed-loop prediction error. This work develops a data-age-aware disturbance-observer model predictive controller (DA-DOB-MPC) for a low-inertia isolated microgrid comprising a dispatchable unit and battery energy storage. A local power-balance observer reconstructs the net-load disturbance, while a timestamp-driven predictor propagates delayed remote states and tightens the input envelope as data age increases. The resulting controller preserves a fixed 20-ms sampling interval and a fixed projected-gradient iteration budget. It is evaluated against PI control and conventional MPC under nominal measurements, 100-ms delay, three packet-loss bursts, measurement noise, and a 30-plant Monte Carlo set with ±20% parameter variation. Under impaired communication, DA-DOB-MPC reduces integral absolute frequency error from 8.0692 Hz·s for PI and 2.3774 Hz·s for conventional MPC to 0.7147 Hz·s. The Monte Carlo median IAE is 0.7103 Hz·s, compared with 8.0424 and 2.1606 Hz·s, respectively. These results support a bounded, model-based use of local disturbance reconstruction; they do not establish hardware-level robustness, which remains to be verified experimentally.*
KEYWORDS: battery energy storage; communication delay; disturbance observer; islanded microgrid; load-frequency control; model predictive control; packet loss.

Date of Submission: 02-09-2026 Date of acceptance: 12-09-2026

NOMENCLATURE

Symbol	Description	Unit
M	Equivalent inertia coefficient	s
D	Frequency-sensitive damping	p.u./Hz
R	Governor droop	Hz/p.u.
Tg, Tt, Tb	Governor, turbine, and BESS time constants	s
a(k)	Age of the most recent valid remote sample	s
d-hat(k)	Estimated net-load disturbance	p.u.
Np	Prediction horizon	samples
um, ub	Diesel and BESS commands	p.u.

I. INTRODUCTION

Low-inertia islanded microgrids must balance volatile renewable generation and load without support from a strong utility grid. Converter-interfaced resources can react rapidly, but their limited stored energy and the slower dynamics of dispatchable generation make secondary frequency regulation a constrained multivariable problem. Predictive control is attractive because it can allocate fast and slow responses explicitly. Centralized and distributed MPC studies have demonstrated transient frequency control, scalable coordination, and active/reactive constraint handling [1]-[4]. These results, however, normally depend on a sufficiently current state vector and a credible disturbance description.

Communication quality is part of the plant seen by a digital controller. Fixed delay, asynchronous sampling, and packet loss create a discrepancy between the state used by the optimizer and the physical state. Event-triggered, predictive, observer-based, and resilient secondary-control studies address complementary aspects of this problem [5]-[12]. Their common lesson is that nominal stability cannot be extrapolated to stale information without specifying the estimator, the time base, and the behavior adopted during missing updates. A controller that simply holds the last packet may continue solving a mathematically valid optimization problem around a physically obsolete initial condition.

This study asks a narrower question: can a local power-balance disturbance observer and an explicit data-age variable preserve the useful constraint-handling properties of MPC during realistic telemetry impairment? Three contributions are developed. First, the net-load disturbance is reconstructed from locally available frequency and actuator states, avoiding dependence on a continuously delivered remote load measurement. Second, the latest remote state is propagated to the current instant, and its age tightens the admissible command set. Third, the controller is assessed under information impairment and simultaneous plant uncertainty, with all algorithms, disturbances, limits, and performance indices reported. The proposed method is not described as a digital twin; it is a control-oriented observer-predictor whose assumptions can be checked directly.

II. MICROGRID MODEL AND COMMUNICATION PROCESS

The incremental model contains frequency deviation Δf, mechanical power ΔPm, governor state ΔPg, and BESS power ΔPb. A positive disturbance ΔP_L denotes a net-load increase. The active-power balance and actuator dynamics are

$$M\frac{d\Delta f}{dt} = \Delta P_m + \Delta P_b - \Delta P_L - D\Delta f, \tag{1}$$

$$T_t\frac{d\Delta P_m}{dt} = -\Delta P_m + \Delta P_g, \qquad T_g\frac{d\Delta P_g}{dt} = -\Delta P_g - \frac{\Delta f}{R} + u_m, \tag{2}$$

$$T_b\frac{d\Delta P_b}{dt} = -\Delta P_b + u_b. \tag{3}$$

With $x = [\Delta f, \Delta Pm, \Delta Pg, \Delta Pb]^{\mathrm{T}}, u = [um, ub]^{\mathrm{T}}$, and $d = \Delta P_L$, exact zero-order-hold discretization gives

$$\mathbf{x}(k+1) = \mathbf{A}_d\mathbf{x}(k) + \mathbf{B}_d\mathbf{u}(k) + \mathbf{E}_d d(k). \tag{4}$$

Remote supervisory packets are timestamped. If kℓ is the index of the latest packet accepted at sample k, the data age is $a(k) = (k - k\ell)Ts$. The test channel has a constant 100-ms transport delay and packet-loss intervals of 0.4, 0.3, and 0.5 s. Local frequency and actuator states remain available at the controller location; only the remote state/disturbance packet is delayed. This separation is important because it states exactly which information survives a network outage.

Data-Age-Aware Disturbance-Observer MPC Architecture

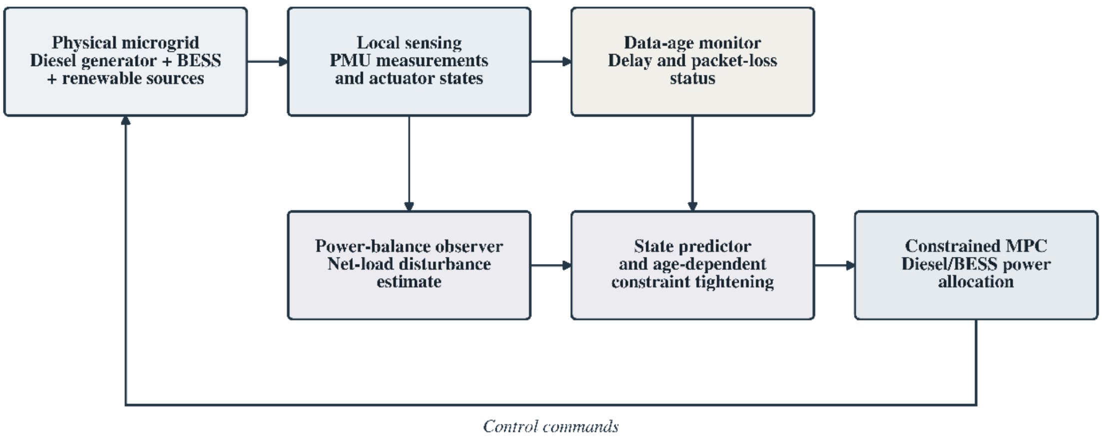

Fig. 1. Proposed local-observer, data-age monitor, predictor, and constrained-MPC architecture

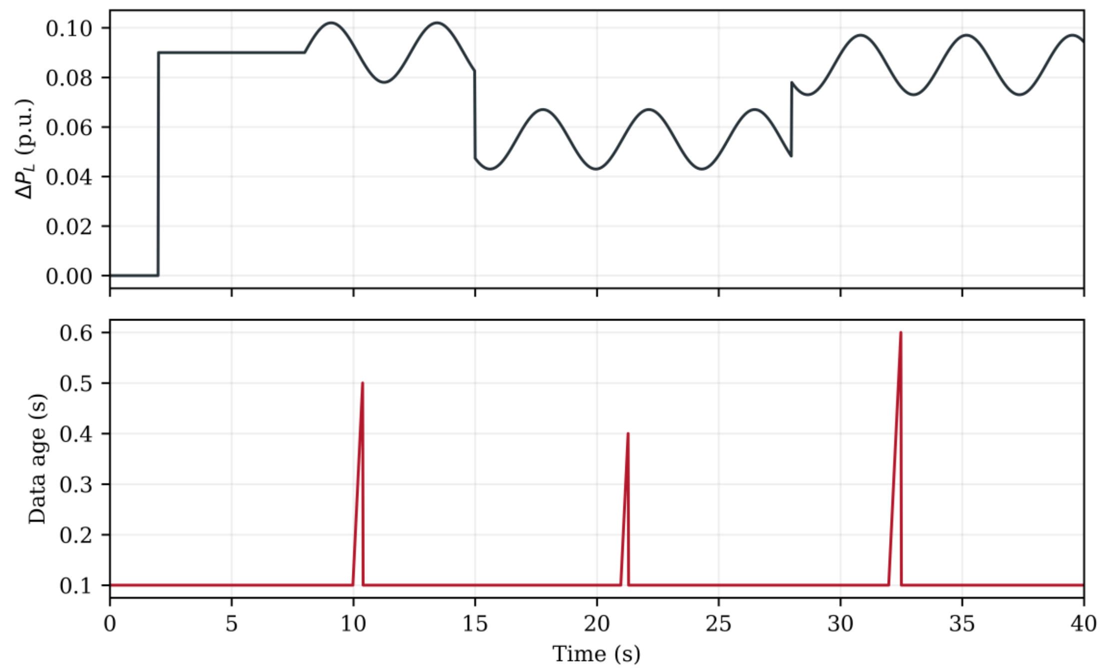

Fig. 2 Net-load disturbance and age of the most recently accepted remote packet

III. DATA-AGE-AWARE DISTURBANCE-OBSERVER MPC

From (1), the net-load disturbance can be reconstructed using local measurements. Direct differentiation of frequency is noise sensitive, so the raw estimate is saturated and passed through a first-order filter:

$$d_{\text{raw}}(k) = \Delta P_m(k) + \Delta P_b(k) - D\Delta f(k) - M\frac{\Delta f(k)-\Delta f(k-1)}{T_s}, \quad (5)$$

$$\hat{d}(k) = \beta\hat{d}(k-1) + (1-\beta)\text{sat}[d_{\text{raw}}(k)], \qquad 0<\beta<1. \quad (6)$$

The expression is a compact power-balance disturbance observer rather than a learned estimator. Its bandwidth is set by β=0.90. More elaborate extended-state observers may improve noise rejection [5], [14], but the low-order form makes the information path and tuning reproducible.

The latest accepted remote state $x(k_\ell)$ is propagated over n_a=round[a(k)/Ts] samples with the nominal model, previously issued input, and d-hat(k):

$$\mathbf{x}_p(k \mid k_\ell) = \mathbf{A}_d^{n_a}\mathbf{x}(k_\ell) + \sum_{j=0}^{n_a-1}\mathbf{A}_d^{j}\left[\mathbf{B}_d\mathbf{u}(k-1) + \mathbf{E}_d\hat{d}(k)\right]. \quad (7)$$

The locally measured frequency replaces the first component of the propagated state. This prevents a stale remote frequency value from overriding a current local PMU measurement. The stacked prediction over Np samples is $X = \Phi x - p + \Gamma U + \Gamma dD$. The control sequence is found from

$$\min_{\mathbf{U}} \mathbf{X}^{\mathrm{T}}\mathbf{Q}\mathbf{X} + \mathbf{U}^{\mathrm{T}}\mathbf{R}\mathbf{U}, \qquad \text{subject to} \quad |u_i| \le u_{\max}[a(k)]. \quad (8)$$

$$u_{\max}(a) = \max\left\{u_{\min},\ u_0 - k_a\min\left(\frac{a}{a_{\max}}, 1\right)\right\}. \quad (9)$$

Constraint tightening is not claimed to form a complete robust positively invariant tube. It is an age-dependent safety margin motivated by robust MPC principles [13], [17]. Here $u0 = 0.18 p.u.$, $umin = 0.11 p.u., ka = 0.08 p.u., Np = 15$, and 35 warm-started projected-gradient iterations are executed at every 20-ms sample. Hence the computation has a deterministic iteration budget. The first optimized pair is applied and the horizon is shifted at the next sample.

Table 1. Plant, observer, optimizer, and robustness-test parameters

Parameter	Value	Parameter	Value
Base power/frequency	1 MW / 50 Hz	M, D	4.5 s / 0.8 p.u./Hz
R, Tg, Tt	2.4 / 0.18 s / 0.45 s	Tb, Ts	0.08 s / 0.02 s
Prediction horizon	15 samples	PG iterations	35
Input envelope	±0.18 p.u.	Minimum tightened limit	±0.11 p.u.
Observer filter β	0.90	Monte Carlo range	±20%

IV. SIMULATION DESIGN AND PERFORMANCE INDICES

The 40-s disturbance comprises a 0.09-p.u. step at 2 s, a reduction of 0.035 p.u. at 15 s, a further rise of 0.03 p.u. at 28 s, and a 0.012-p.u., 0.23-Hz oscillation after 8 s. PI, conventional MPC, and DA-DOB-MPC use the same physical plant and actuator limits. Conventional MPC receives the delayed, held state and net-load packet. DA-DOB-MPC receives the same packet but reconstructs disturbance and propagates stale states as defined in (5)-(7). No controller receives future disturbance samples.

Peak |Δf|, maximum ROCOF, integral absolute error (IAE), root-mean-square error (RMS), and integral absolute command are reported. Since the oscillatory component prevents a single permanent settling time from being informative, no settling-time ranking is used. The uncertainty experiment samples M, D, R, Tg, Tt, and Tb independently from uniform ±20% intervals. Thirty plants are evaluated with the same network impairment and without retuning.

V. RESULTS AND DISCUSSION

A. Nominal measurements

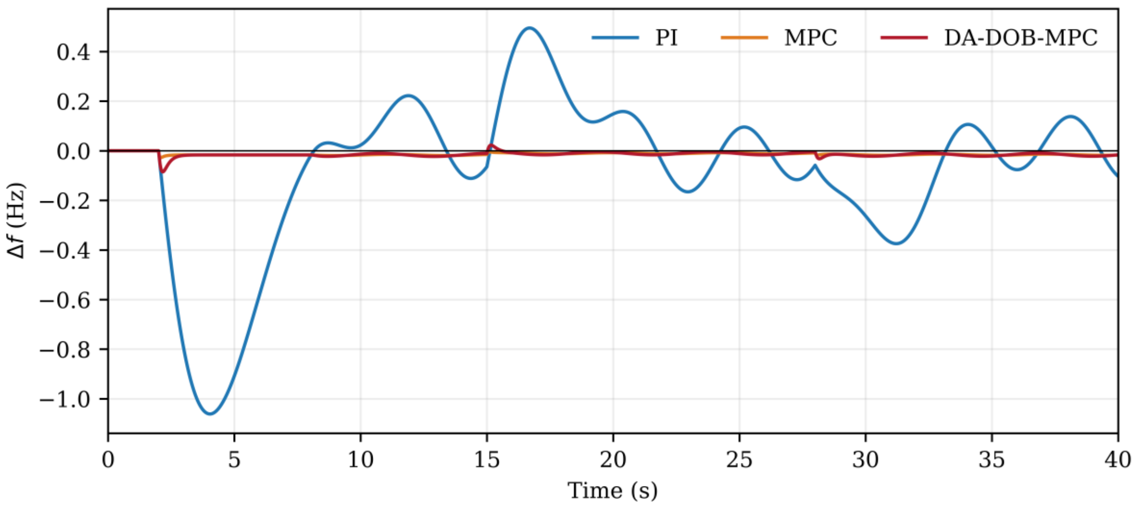

Fig. 3. Nominal frequency responses under identical disturbance and actuator limits

Conventional MPC produces the smallest nominal peak (0.0277 Hz), while DA-DOB-MPC gives a 0.0851-Hz peak because the disturbance filter deliberately rejects abrupt derivative estimates. The nominal IAEs of MPC and DA-DOB-MPC are close: 0.5443 and 0.5843 Hz·s, respectively, compared with 8.0692 Hz·s for PI. The result exposes the cost of observer filtering rather than hiding it: the proposed method is not superior when communication is ideal and the disturbance packet is current.

B. Delayed and missing telemetry

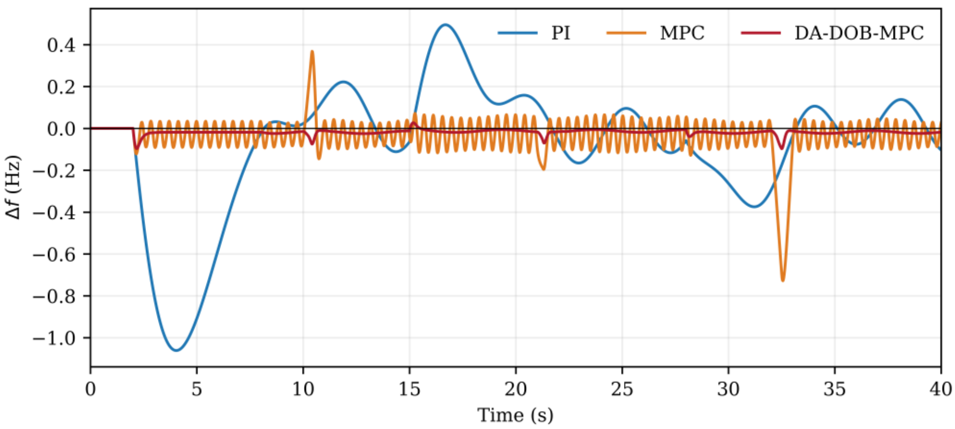

Fig. 4 Frequency responses with 100-ms delay, measurement noise, and three packet-loss bursts

Table 2. Performance under 100-ms delay and burst packet loss

Controller	Peak |Δf| (Hz)	ROCOF (Hz/s)	IAE (Hz·s)	RMS (Hz)
PI	1.0612	0.9982	8.0692	0.3165
MPC	0.7281	2.5839	2.3774	0.0982
DA-DOB-MPC	0.0971	0.9982	0.7147	0.0214

The impaired channel changes the ranking. Conventional MPC continues to optimize around held information and reaches a 0.7281-Hz peak with ROCOF of 2.5839 Hz/s. DA-DOB-MPC limits the peak to 0.0971 Hz and IAE to 0.7147 Hz·s. Relative to conventional MPC, these reductions are 86.7% and 69.9%, respectively; relative to PI, they are 90.8% and 91.1%. The improvement is caused by two explicit mechanisms: the local power-balance estimate prevents the disturbance channel from freezing, and state propagation reduces the age-induced initialization error. PI is less sensitive to remote packets but cannot coordinate the fast and slow channels as effectively.

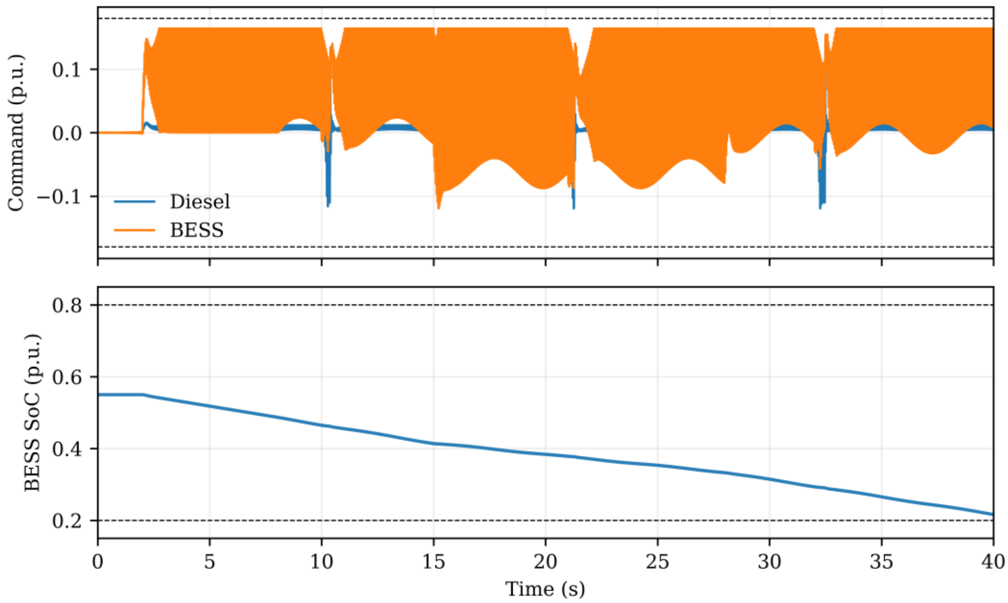

Fig. 5 Proposed diesel/BESS commands and illustrative BESS state-of-charge trajectory

The command trajectories remain inside the instantaneous envelope, and the illustrative BESS state of charge remains within 0.2-0.8 p.u. for the assumed 8-p.u.-s normalized energy capacity. This SoC calculation is an energy-consistency check, not an electrochemical battery model. Converter current limits, efficiency variation, thermal aging, and SoC estimation error must be added before hardware claims are made.

C. Parameter uncertainty

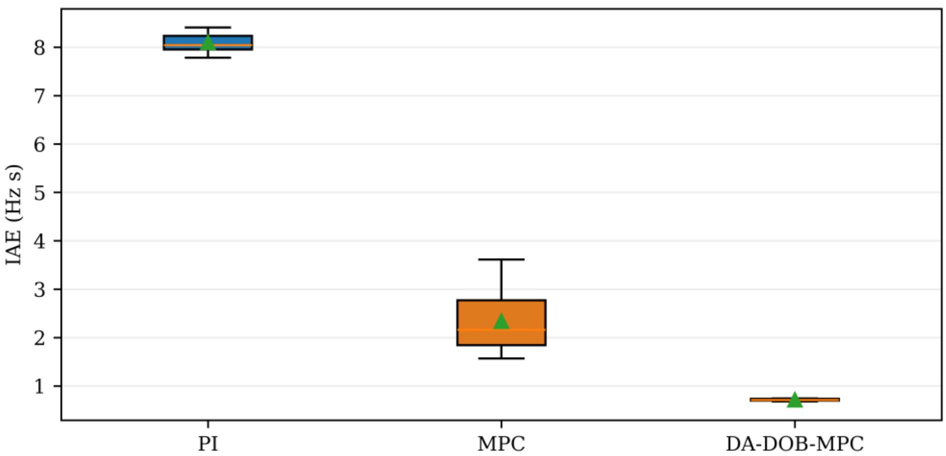

Fig. 6 IAE distribution for 30 uncertain plants under the impaired communication case

Table 3. Monte Carlo IAE statistics (Hz·s)

Controller	Median IAE	Interquartile interval	Worst IAE
PI	8.0424	7.9550-8.2337	8.4069
MPC	2.1606	1.8419-2.7708	3.6135
DA-DOB-MPC	0.7103	0.6941-0.7335	0.7414

The proposed distribution is both lower and narrower. Its worst IAE, 0.7414 Hz·s, remains below the best quartile of conventional MPC. This is evidence of numerical robustness over the stated independent parameter box, not a proof for arbitrary nonlinearities or correlated uncertainty. Governor deadband, generation-rate limits, converter switching, battery degradation, clock drift, and adversarial timestamp manipulation are outside the present plant model.

VI. IMPLEMENTATION IMPLICATIONS AND LIMITATIONS

The method requires local frequency and actuator-state availability during remote-link interruption. If these signals share the same failed network, the disturbance reconstruction in (5) is unavailable and the controller must revert to a separately validated local droop/PI mode. Timestamp authentication is also necessary: an incorrect but plausible timestamp can cause inappropriate propagation and constraint tightening. IEEE microgrid-controller guidance emphasizes defined functional boundaries and transition behavior [16]; the data-age variable should therefore be implemented as a monitored safety signal, not merely as diagnostic metadata.

The projected-gradient solver has a fixed iteration count, yet worst-case processor timing has not been measured. A credible next stage is processor-in-the-loop timing followed by controller-HIL tests with packet reordering, clock offset, quantization, and converter saturation. The observer gain and age-tightening slope should then be tuned against a specified noise spectrum and network service envelope. Learning may support this tuning, but it should not replace the explicit constraints or the last-known-good fallback.

VII. CONCLUSION

A data-age-aware disturbance-observer MPC has been formulated for diesel-BESS frequency regulation in a low-inertia islanded microgrid. The method reconstructs net-load imbalance locally, propagates delayed supervisory states, and reduces the command envelope as information becomes stale. Conventional MPC remains marginally better under ideal communication, whereas the proposed controller substantially reduces peak deviation and IAE when 100-ms delay, packet-loss bursts, measurement noise, and ±20% plant variation are introduced. The conclusion is conditional on local measurement availability and the reported linear model. Hardware timing, nonlinear actuator effects, authenticated timestamps, and bumpless fallback remain necessary before deployment.

REFERENCES

[1] T. Heins, M. Joševski, S. K. Gurumurthy, and A. Monti, "Centralized model predictive control for transient frequency control in islanded inverter-based microgrids," IEEE Transactions on Power Systems, vol. 38, no. 3, pp. 2641-2652, 2023. doi: 10.1109/TPWRS.2022.3189958.

[2] M. Moritz, T. Heins, S. K. Gurumurthy, M. Joševski, I. Jahn, and A. Monti, "Distributed model predictive frequency control of inverter-based power systems," IEEE Access, vol. 12, pp. 53250-53265, 2024. doi: 10.1109/ACCESS.2024.3387369.

[3] G. Ferro, M. Robba, and R. Sacile, "A fully distributed robust MPC approach for frequency and voltage regulation in smart grids with active and reactive power constraints," IEEE Transactions on Systems, Man, and Cybernetics: Systems, vol. 54, no. 11, pp. 6657-6669, 2024. doi: 10.1109/TSMC.2024.3426083.

[4] J. Xiao, L. Wang, Y. Wan, P. Bauer, and Z. Qin, "Distributed model predictive control-based secondary control for power regulation in AC microgrids," IEEE Transactions on Smart Grid, vol. 15, no. 6, pp. 5298-5308, 2024. doi: 10.1109/TSG.2024.3409154.

[5] P. Ge, X. Dou, X. Quan, Q. Hu, W. Sheng, Z. Wu, et al., "Extended-state-observer-based distributed robust secondary voltage and frequency control for an autonomous microgrid," IEEE Transactions on Sustainable Energy, vol. 11, no. 1, pp. 195-205, 2020. doi: 10.1109/TSTE.2018.2888562.

[6] Y. Yu, G.-P. Liu, and W. Hu, "Coordinated distributed predictive control for voltage regulation of DC microgrids with communication delays and data loss," IEEE Transactions on Smart Grid, vol. 14, no. 3, pp. 1708-1722, 2023. doi: 10.1109/TSG.2022.3208946.

[7] Y. Xia, Y. Xu, Y. Wang, S. Mondal, S. Dasgupta, and A. K. Gupta, "Optimal secondary control of islanded AC microgrids with communication time-delay based on multi-agent deep reinforcement learning," CSEE Journal of Power and Energy Systems, vol. 9, no. 4, pp. 1301-1311, 2023. doi: 10.17775/CSEEJPES.2021.08680.

[8] B. Zhang, C. Dou, D. Yue, Z. Zhang, and T. Zhang, "A packet loss-dependent event-triggered cyber-physical cooperative control strategy for islanded microgrid," IEEE Transactions on Cybernetics, vol. 51, no. 1, pp. 267-282, 2021. doi: 10.1109/TCYB.2019.2954181.

[9] X. Li, C. Wen, C. Chen, and Q. Xu, "Adaptive resilient secondary control for microgrids with communication faults," IEEE Transactions on Cybernetics, vol. 52, no. 8, pp. 8493-8503, 2022. doi: 10.1109/TCYB.2021.3070820.

[10] S. Arunima and B. Subudhi, "An observer-based distributed cooperative event-triggered control scheme for an AC microgrid," IEEE Transactions on Smart Grid, vol. 15, no. 6, pp. 5321-5330, 2024. doi: 10.1109/TSG.2024.3412728.

[11] Y. Chen, D. Qi, Z. Li, Z. Wang, X. Yang, and J. Zhang, "Distributed event-triggered control for frequency restoration in islanded microgrids with reduced trigger condition checking," CSEE Journal of Power and Energy Systems, vol. 10, no. 5, pp. 2156-2165, 2024. doi: 10.17775/CSEEJPES.2020.05730.

[12] Z. Sajjadinezhad and N. M. Dehkordi, "Fully distributed adaptive event-triggered control with delay-aware dynamic thresholds for islanded AC microgrids," Scientific Reports, vol. 15, Art. no. 27900, 2025. doi: 10.1038/s41598-025-13955-8.

[13] D. Q. Mayne, M. M. Seron, and S. V. Raković, "Robust model predictive control of constrained linear systems with bounded disturbances," Automatica, vol. 41, no. 2, pp. 219-224, 2005. doi: 10.1016/j.automatica.2004.08.019.
[14] R. Madoński and P. Herman, "Survey on methods of increasing the efficiency of extended state disturbance observers," ISA Transactions, vol. 56, pp. 18-27, 2015. doi: 10.1016/j.isatra.2014.11.008.
[15] M. Schwenzer, M. Ay, T. Bergs, and D. Abel, "Review on model predictive control: An engineering perspective," The International Journal of Advanced Manufacturing Technology, vol. 117, pp. 1327-1349, 2021. doi: 10.1007/s00170-021-07682-3.
[16] IEEE Standard for the Specification of Microgrid Controllers, IEEE Std 2030.7-2017, 2018. doi: 10.1109/IEEESTD.2018.8340204.
[17] J. B. Rawlings, D. Q. Mayne, and M. M. Diehl, Model Predictive Control: Theory, Computation, and Design, 2nd ed. Santa Barbara, CA, USA: Nob Hill Publishing, 2017. URL: https://sites.engineering.ucsb.edu/~jbraw/mpc/.
[18] J. Zhang, B. Zhou, H. Zhang, and D. Yang, "Fully distributed event-triggered secondary control for islanded microgrid restoration with communication link faults," IEEE Transactions on Automation Science and Engineering, vol. 23, pp. 2465-2474, 2026. doi: 10.1109/TASE.2025.3650604.